Phytochemistry Letters 60 (2024) 134–142

Contents lists available at ScienceDirect

Phytochemistry Letters

journal homepage: www.elsevier.com/locate/phytol

Styryllactones in the leaves of *Goniothalamus lanceolatus* Miq., molecular networking and their anti-dengue activity *In vitro* and *In silico*

Nor Nadirah Abdullah [a,b], Adlin Afzan [c], Nur Hana Jelas [c], Mohd Ridzuan Mohd Abd Razak [c], Nurulfazlina Edayah Rasol [a,b], Syahrul Imran Abu Bakar [a,b], Nur Vicky Bihud [a,b], Lam Kok Wai [d], Murizal Zainol [c], Fasihuddin Badruddin Ahmad [e], Geoffrey A. Cordell [f,g], Nor Hadiani Ismail [a,b,*]

[a] *Atta-ur-Rahman Institute for Natural Products Discovery, Universiti Teknologi MARA, 42300 Puncak Alam, Selangor, Malaysia*
[b] *Faculty of Applied Sciences, Universiti Teknologi MARA, 40450 Shah Alam, Selangor, Malaysia*
[c] *Herbal Medicine Research Centre, Institute Medical Research, National Institute of Health, No.1 Jalan Setia Murni U13/52, Seksyen U13, 40170 Shah Alam, Selangor, Malaysia*
[d] *Faculty of Pharmacy, Universiti Kebangsaan Malaysia, Jalan Raja Muda Abdul Aziz, 50300 Kuala Lumpur, Malaysia*
[e] *Department of Chemistry, Faculty of Resources Science and Technology, Universiti Malaysia Sarawak, 94300 Kota Samarahan, Sarawak, Malaysia*
[f] *Natural Products Inc., Evanston, Illinois 60201, United States of America*
[g] *Department of Pharmaceutics, College of Pharmacy, University of Florida, Gainesville, Florida 32610, United States of America*

ARTICLE INFO

Keywords:
Goniothalamus lanceolatus
Styryllactones
Dengue virus
Plaque assay
QRT-PCR
Molecular networking
Docking

ABSTRACT

Due to dengue fever's swift global expansion and the lack of effective antiviral remedies, it is crucial to discover and develop new antiviral drugs. The study aimed to assess the antiviral potential of the extract and fractions from the leaves of *Goniothalamus lanceolatus* Miq. (Annonaceae). New Guinea C strain DENV-2, at a multiplicity of infection of 0.4, was used to infect Vero cells. The assessment of antiviral effectiveness was conducted through the plaque reduction assay. Deep metabolome analysis of the active fraction identified nine styryllactones based on reference standards and eighteen styryllactones were further annotated through a molecular database search. One new 2*H*-tetrahydropyran derivative, 3-*epi*-goniothalesdiol A (**19**), together with seven known styryllactones (**8**, **11**, **14**, **16**, **17**, **18**, and **22**) were isolated from the leaves of *G. lanceolatus*. The active bis-styryllactone goniolanceolatin A (**22**) with the highest selectivity index (SI) underwent further evaluation using quantitative reverse transcription qRT-PCR to determine the viral RNA level. The qRT-PCR data showed that the IC_{50} value for the active compound was 5.07 μg/mL, and its corresponding SI value was 5.30. Following comprehensive docking studies, the bis-styryllactone derivative **22** showed potential binding interactions with crucial amino acids of the Envelope (E) of DENV proteins comparable to those of ribavirin.

1. Introduction

Dengue infections are caused by the dengue virus (DENV) which belongs to the genus *Flavivirus* in the family Flaviviridae and is transmitted by infected female *Aedes aegypti* mosquitoes. The virus has four, antigenically-related serotypes identified as DENV-1, DENV-2, DENV-3, and DENV-4. Infection from this virus may be asymptomatic or can lead to undifferentiated fever involving dengue fever (DF), dengue hemorrhagic fever (DHF), and dengue shock syndrome (DSS) (Gubler, 1998; Kalayanarooj, 2011). Based on the World Health Organization (WHO) (2022) assessment, about half of the world's population is presently at risk from infection, and it is believed that there are between 100–400 million cases of dengue worldwide every year. Dengue fever has the highest prevalence rate among communicable diseases in Malaysia, with 397 cases per 100,000 population (Mashudi et al., 2022). At present, there is no specific treatment to combat the global ravages of this disease (Paz-Bailey et al., 2021).

In the development and discovery of new antiviral drugs, medicinal plants, and plant-derived metabolites play an important role in treating a variety of infectious diseases (Kwon et al., 2010; Yasuhara-Bell et al., 2010). The genus *Goniothalamus* (Blume) Hook. f. & Thomson belongs to the Annonaceae family, and *Goniothalamus* species are rich in styryllactones, acetogenins, alkaloids, and flavonoid derivatives (Zandi et al., 2009). Two metabolite classes are exhibiting anti-cancer effects

* Corresponding author at: Atta-ur-Rahman Institute for Natural Products Discovery, Universiti Teknologi MARA, 42300 Puncak Alam, Selangor, Malaysia.
E-mail address: norhadiani@uitm.edu.my (N.H. Ismail).

https://doi.org/10.1016/j.phytol.2024.01.012
Received 16 July 2023; Received in revised form 21 December 2023; Accepted 24 January 2024
Available online 9 February 2024

from plants in this genus, styryllactones and the acetogenins (Zandi et al., 2009; Mahiwan et al., 2013). Previous studies on extracts and isolates from *Goniothalamus* species have also shown promising activity against infective agents, including malarial parasites, dengue virus (Ichino et al., 2006; Prawat et al., 2012), and other viruses (Cao et al., 1998; Ichino et al., 2006; Prawat et al., 2012; Claire et al., 2013). Recently, styryl pyrone derivatives (SPD) from the roots of *G. umbrosus* J. Sinclair were reported to show potential antiviral activity against DENV type-2 (Abd Wahab and Ibrahim, 2022). The core skeleton of styryllactones namely goniothalamin, was reported to inhibit DENV-2 E protein activity through a reduction in the expression of the DENV-2 E gene and protein at various stages of viral replication, as well as possesses the capacity to reduce the virus that infects new cells (Abd Wahab et al., 2022).

G. lanceolatus Miq., also known in Malaysia as *Selukai* or *Getimang*, is an endemic plant from the rainforest in Sarawak, Malaysia, where the indigenous population uses the leaves as a mosquito repellent, and to treat fevers, colds, and skin diseases (Wiart, 2007). Styryllactones, bis-styryllactones, acetogenins, and alkaloid derivatives from the stem-bark and roots of *G. lanceolatus* were cytotoxic against several human cell lines (Rasol et al., 2018; Rasol et al., 2018; Bihud et al., 2019). In addition, the isolates from the roots of *G. lanceolatus* were reported to possess significant antimalarial activity against both chloroquine-sensitive (3D7) and chloroquine-resistant (K1) strains of P. falciparum with excellent selective indices ($IC_{50} = 2.7$ μg/mL, SI = 140; $IC_{50} = 1.7$ μg/mL, SI = 236) (Kaharudin et al., 2020). In this study, the most active fractions derived from the leaves of *G. lanceolatus* and comprising mainly styryllactones, were evaluated against DENV-2 (NGC strain) replication through both *in vitro* and *in silico* assessments.

Currently, the high sensitivity advantage of HR-MS enables the in-depth investigation of the metabolomic profile of the contained natural products, which simplifies the disclosure of both known and new bioactive compounds (Nothias et al., 2018; Yang et al., 2022). Several open-source platforms are available for analysing the high-throughput HR-MS data generated. The Global Natural Product Social Molecular Networking (GNPS MN) (2016) platform provides advanced visualization of the relationships between thousands of LC-MS features and their distribution in multiple samples. With the availability of public databases and the crowdsourcing of spectral data within the GNPS platform, known compounds can be expected to be identified. Another open-source software, SIRIUS (2022), is a sophisticated compound annotation tool that further enhances the identification coverage through the application of computational *in silico* methods. This software uses a Compound Structure Identification (CSI:FingerID) module, in which fragmentation trees are constructed from the mass spectral data to predict molecular fingerprint relationships. The matching of these fingerprints coalesces with the molecular fingerprints computed from the various molecular structure databases.

To annotate the major metabolites present in the most active fraction of *G. lanceolatus*, a UHPLC-ESI-Orbitrap-HRMS/MS system combined with feature-based molecular networking-Global Natural Products Social (FBMN-GNPS) and *in silico* annotation using the SIRIUS bioinformatic tool was employed (Dührkop et al., 2015; Böcker et al., 2016). Even though the bioprospecting of medicinal plants approach has been replaced by modern techniques using targeted tools for identifying compounds with biological potential, the integration of *in vitro* and *in silico* evaluations permits the identification of promising antiviral metabolites, as well as exploring their potential mechanism of action (Trujillo-Correa et al., 2019).

2. Experimental

2.1. Plant material

The leaves of *G. lanceolatus* Miq. were collected by Prof Fasihuddin Badruddin Ahmad in June 2012 from the outskirts of the small town of Lundu in Sematan Sarawak, Malaysia. It was identified by the late Prof Dr. Kamaruddin Mat Salleh (Botany Department, Faculty of Science and Technology, Universiti Kebangsaan Malaysia) and a voucher specimen (FBAUMS 108) was deposited in the Herbarium Department of the Universiti Malaysia Sarawak, Kuching, Sarawak, Malaysia.

2.2. Plant extraction, fractionation, and sample preparation

Dried and ground leaves (2.04 kg) of *G. lanceolatus* were macerated with solvents of increasing polarity, starting from hexane, dichloromethane, and methanol successively for 3 days at room temperature. The maceration was repeated thrice for each solvent and approximately 10–15 L of solvent was used for each extraction. The dichloromethane extract was evaporated on a rotary evaporator at 45 °C to afford the GLLD extract (49.30 g) extract. Based on the initial biological activity assessment, the dichloromethane leaves extract (GLLD) (46.00 g) was fractionated by Medium Pressure Liquid Chromatography (MPLC) on an ODS column eluted with a MeOH: H_2O (30:70 to 100:0) gradient system from 0–70 min to afford six fractions (F1-F6).

The *G. lanceolatus* fractions (10 mg) were pre-treated with a solid phase extraction method (DPA-6S, polyamide, 50 mg/mL, Supelco, USA) to remove tannins using a methanol: water (7:3) solvent system and the eluent evaporated at 45 °C. Stock solutions (1000 μg/mL) of the sample and the isolated compounds were prepared in HPLC grade methanol: Milli-Q water (H_2O) (7:3). The isolated compounds were further diluted to a concentration of 10 μg/mL.

2.3. Isolation and characterization of the compounds present in the active fraction

Fraction F2 (1.5 g) was further chromatographed using Preparative High-Pressure Liquid Chromatography (PHPLC) to yield eight subfractions (P1-P8). The solvent system used was H_2O (A) and MeOH (B) and the gradient was as follows: 30% B - 55% B for 15 min; 55% B - 100% B from 15–19 min; 100% B from 19–24 min; 100% B - 30% B from 24–26 min; and finally, a 4 min column equilibration with 30% B was applied. Further purification was performed on subfraction P2 using reversed-phase Recycling HPLC on a JAIGEL-ODS-AP-30, SP-120–15 column, H_2O: MeOH (3:7, v/v) as a mobile phase at a flow rate of 4.0 mL/min to generate **8** (39.2 mg) and **17** (3.1 mg).

Subfraction P3 was subjected to reversed-phase Recycling HPLC using H_2O: MeOH (65:35, v/v) at a flow rate of 4 mL/min to afford **11** (16.4 mg) and **14** (3.5 mg). Further separation of subfraction P4 by reversed-phase Recycling HPLC using system solvent of H_2O: MeOH (60:40, v/v) afforded **16** (2.3 mg). In addition, compounds **18** (4.7 mg), **19** (5.1 mg), and **22** (5.5 mg) were obtained from subfraction P6 through reversed-phase Recycling HPLC at the same flow rate and using the isocratic solvent system of H_2O: MeOH (55:45, v/v).

2.4. MS/MS-based dereplication (UHPLC-Orbitrap-MS/MS conditions)

Fraction 2 (F2) from the GLLD extract was analyzed using a Vanquish Horizon Ultra-High-Performance Liquid Chromatograph (UHPLC) coupled to a Q-Exactive Orbitrap™ mass spectrometer (Thermo Fisher Scientific™, Waltham, MA, USA) interfaced with an electrospray (ESI) ionization system. The LC separation was performed on a Waters™ BEH UPLC C18 column (2.1 ×100 mm, 1.6 μm, Waters, Waltham, MA, USA), maintained at 40 ºC throughout the analysis. The mobile phase consisted of 0.1% formic acid in Milli-Q water (A) and 0.1% formic acid in acetonitrile (B). The liquid chromatography gradient was as follows: 5% – 100% B from min 0.00–20.00; flushing with 100% B from min 20.00–24.00; 100%– 5% B from min 24.00–24.10; and finally, 2.9 min column equilibration with 5% B. The flow rate was 0.3 mL/min throughout the analysis. The injection volume was 1 μL (1000 μg/mL in MeOH:H_2O (7:3)), and the sample tray temperature was maintained at 10 °C. The high-resolution mass spectrometer (HRMS) was operated at a

resolution of 70,000 for the full scan and 17,500 orbitrap resolutions for the data-dependent MS/MS scan. The heated ESI source was optimized with 3.50 kV static spray voltage; 320 °C capillary temperature, 35 L/min sheath gas flow; 10 L/min auxiliary gas; and 55% S-lens RF. The HR-MS data were acquired at a mass scan range from *m/z* 100 to 1500 as centroid spectra in the positive ion mode (ESI^+).

2.5. Molecular network generation

For application of the Feature-Based Molecular Networking-Global Natural Products Social (FBNM-GNPS), the high-resolution mass spectral data were processed using MZmine 3.1.0. The MZmine workflow begins with detecting the noise level threshold (MS level 1:1.0E6; MS level 2:1.0E0) with a centroid detector. The chromatogram builder was used with a minimum time span of 0 min and a *m/z* tolerance of 0.01 *m/z* or 5.0 ppm. The chromatogram deconvolution parameters were set as follows: peak duration range of 0–2 (min) and minimum feature height of 1.0E6. The deisotoped parameter using an isotopic peak grouper with the following parameters: *m/z* tolerance: 0.01 *m/z* or 5.0 ppm; retention time tolerance: 0.1 absolute (min); maximum charge: 2; and representative isotope: most intense. Then, the.mgf file and quant table data were exported from MZmine to the GNPS molecular networking platform (https://gnps.ucsd.edu/ProteoSAFe/static/gnps-splash.jsp) for molecular network construction and metabolite annotation. The spectral library search was performed using 0.02 Da ion mass and fragment ion tolerance. The score threshold was set at 0.70 for advanced spectral matching with the MS/MS libraries. The resulting molecular network is available at (https://gnps.ucsd.edu/ProteoSAFe/status.jsp?task=d5e08add9da24455b260df0402f55e88). The molecular network was further visualized through Cytoscape software version 3.5 (Shannon, 2003).

2.6. Compound annotations

The.mgf file containing the spectral data of all 279 MS features generated from the MZmine analysis was used for *in silico* annotations using Sirius 5 open-source software (https://boecker-lab.github.io/docs.sirius.github.io/). The first step in this annotation workflow is molecular formula determination, for which the mass tolerance was set at 15 ppm for the elements carbon, hydrogen, oxygen, and nitrogen. In this step, it was crucial to set the correct adduct for more precise molecular formula prediction. The CSI: Finger ID search was used to annotate the chemical structure. In this second step, the software attempts to explain all of the MS/MS fragment ions by generating an MS/MS fragmentation tree. Subsequently, the fragmentation tree is used to predict the molecular fingerprint which encodes the structure of the molecule. The predicted molecular fingerprint was then submitted to the molecular databases available within the software. Some of the selected databases related to natural products were the COCONUT and Lotus databases. Additionally, a custom database containing the Smiles strings of isolated compounds reported from the *Goniothalamus* genus was uploaded to the software to provide enhanced confidence in the annotations. This custom database was generated from the *Dictionary of Natural Products* (DNP) database and assessed on UiTM EzAccess using the keyword CHEMnetBASE: Dictionary of Natural Products (https://dnp-chemnetbase-com.ezaccess.library.uitm.edu.my/chemical/ChemicalSearch.xhtml?dswid=9182). For every successful match between the molecular fingerprint predicted based on the spectral data with the molecular fingerprint generated from the molecular database, a score was generated. In this study, only styryllactone annotations having a $>$ 50% similarity score are presented. Finally, the CANOPUS database was analyzed to annotate the MS features by chemical family.

2.7. Cell and dengue virus propagation

African Green Monkey Kidney cells (Vero) were purchased from the American Type Culture Collection (ATCC, No. CCL-81, Chiba, Japan). The Vero cells were maintained at 37 °C in a 5% CO_2 Galaxy 170 S incubator (New Brunswick, Braunschweig, Lower Saxony, Germany) and propagated in Dulbecco's modified Eagle medium (DMEM 10270; Gibco Laboratories, Grand Island, NY, USA) supplemented with 10% FBS and 100 U/mL penicillin G and 100 μg/mL streptomycin. DENV-2 New Guinea C. strain (NGC) (ATCC VR-1584) was cultured and propagated in Vero cells. Plaque assays were used to quantify the titer of the dengue virus (Ferris et al., 2011).

2.8. Cytotoxicity assay (MTT assay)

Vero cells were seeded in 96-well plates in 50 μL media as above at 1×10^4 cell per well and incubated at 37 °C in 5% CO_2. After 24 h, 50 μL of crude extracts, fractions, and isolated compounds at various concentrations (0–200 μg/mL) were added. The plates were incubated for 96 h at 37 °C in 5% CO_2. Cell viability (%) was assessed by adding 50 μL of 0.5% (w/w) 3-[4,5-dimethylthiazol-2-yl]− 2,5-diphenyltetrazolium bromide (MTT, Sigma-Aldrich, St. Louis, MO, USA) solution into each well. After incubation for 4 h, the medium was replaced with 100 μL of dimethyl sulfoxide to solubilize the formazan crystals, and the plates were vortexed vigorously to dissolve the formazan. A microplate spectrophotometer (Bio-Rad; Benchmark Plus, Hercules, CA, USA) was used to measure the absorbance at 560 nm (OD_{560}) (Burleson et al., 1992).

2.9. Virus infection and drug exposures

Vero cells were seeded in a 96-well plate as above. The media was removed and the cells were infected with 100 μL of DENV-2 at 0.4 MOI (diluted with Hank's balanced salt solution, HBSS with 0.4% bovine serum albumin, BSA) for 1 h without CO_2. The plates were agitated every 15 min. The viral medium was replaced by 190 μL of DMEM (10% FBS) and 10 μL of extract or isolated compound with serial dilutions to a final concentration of 3.125–200 μg/mL. Ribavirin (10–160 μg/mL) served as a positive control, and the uninfected cells served as the negative control. The plates were incubated at 37 °C in 5% CO_2, and after 4 days, the plates were stored at − 80 °C until further testing (Burleson et al., 1992).

2.10. Plaque assay

To determine the virus yield after treatment from compound exposure, culture supernatants from the previous compound exposure (with and without various concentrations of crude extract and isolated compounds) were subjected to a plaque assay test. A 10-fold serial dilution of the culture supernatant was added to a monolayer of Vero cells grown in a 6-well plate at 4.5×10^5 cells/well. The plate was incubated at 37 °C without CO2. After one hour, the cell suspension was aspirated from the 6-well plate and complete agarose media (3 mL, 2x DMEM media, and 10% FBS) was overlayed into the 6-well plate. When the agarose had hardened, the plate was incubated at 37 °C in 5% CO_2. Following a six-day incubation period, the cells were fixed by adding 50% TCA (1 mL) onto the agarose media, and the cells were stained using 1% crystal violet (1 mL). The virus plaque was counted using the formula (Ferris et al., 2011):

Pfu/mL = Number of plaques × Reciprocal of dilution × Reciprocal of volume.

Virus Growth (%) =pfu/mL of extract treated infected cells × 100%. pfu/mL non-treated infected cells.

2.11. Detection and quantification of viral RNA

The dengue virus titer in the culture supernatant was determined by viral RNA quantification using reverse transcription quantitative PCR (RT-qPCR). The viral RNA was extracted from the culture supernatant according to the manufacturer's instructions using the QIAamp Viral RNA Mini kit (Qiagen, Germantown, MD, USA). The purified viral RNA

was subjected to RT-qPCR (Applied Biosystems 7500 fast, Foster City, CA, USA) using a QuantiTect® Probe RT-PCR detection kit (Qiagen, Germantown, MD, USA) (Gurukumar et al., 2009). The dengue viral RNA with a known copy number was used as a standard for copy number determination. The thermal cycling profile of this assay was started with a 30 min reverse transcription step at 50 ºC, followed by 15 min of HotStarTaq DNA polymerase activation at 95 ºC, a denaturation step for 15 s at 94 ºC, and combined annealing or extension for 45 cycles of PCR at 60 ºC of annealing for 60 s, at 60.0 ºC.

2.12. Molecular docking

The structures of the compounds isolated from the dichloromethane extract of *G. lanceolatus* leaves were drawn using ChemBioDraw® Ultra 13.0 (CambridgeSoft Corporation, Cambridge, MA, USA). The preparation and energy minimization of the ligands was performed using CHARMm forcefield calculations. The crystal structure of the DENV target proteins was retrieved from the Protein Data Bank. The targeted protein was prepared by removing water and unwanted molecules. The protein-ligand docking studies of the inhibitors with the receptor 1OKE were performed using validated CDOCKER protocol in the Discovery Studio® 3.1 (Accelrys, San Diego, CA, USA).

The docking procedure was validated by redocking the co-crystallized inhibitors as a reference ligand with non-structural E protein using CDOCKER to predict the binding interactions of ligands within the catalytic pockets. Then, the ligands were generated through high-temperature molecular dynamics followed by random rotations and refinement by grid-based (GRID I) simulated annealing and full-force field minimization (Wu et al., 2003). The parameters of the docking experiment were set as follows; the cooling steps were set in 5000 steps to 300 K, while for the heated steps, the temperature of 700 K in 2000 steps was used with the grid extension set to 10 Å. The top ten compounds for each ligand binding pose were ranked and analyzed based on their: 1) type of interaction with the active residues of dengue protein; 2) interaction docking energy value; 3) maximum number of interactions with the active residues, and 4) bond distances. The concept was to select only those compounds that bind with the crucial amino acids in the binding pockets of the dengue protein having a favourable docking energy value.

2.13. Statistical analysis

The statistical analysis was performed using Prism 8.00 for Windows™ (GraphPad Software, San Diego, CA, USA). To determine the CC_{50} and IC_{50} values, a non-linear regression analysis was performed. The selectivity index (SI) value of each extract and compound was determined using the formula SI= CC_{50}/IC_{50}. Each experiment was tested in triplicate.

3. Results and discussion

3.1. Cytotoxic and anti-dengue evaluation of G. lanceolatus Miq. crude extracts and leaves dichloromethane leaf extract fractions

The dichloromethane extract of the leaves (GLLD) of *G. lanceolatus*, was evaluated for *in vitro*, dose-response anti-dengue activity using the plaque reduction assay (Ferris et al., 2011), with the antiviral agent ribavirin as the positive control. (Fig. 1A-C). The toxicity levels of the plant extract, fractions, and isolated compounds were evaluated using the MTT assay in Vero monkey kidney cells, and the 50% cytotoxic concentration (CC_{50}) value determined through dose-response curve analysis. GLLD showed promising antiviral activity against DENV-2 with an IC_{50} value of 4.16 µg/mL and the CC_{50} value was 24.23 µg/mL, resulting in a Selectivity Index (SI) (Likhitwitayawuid et al., 1993; Severson et al., 2008; Abdullah et al., 2021) of 5.82 (Fig. 1A). Six fractions from the GLLD extract were subjected to an MTT test and a dose-dependent plaque reduction assay to evaluate further their antiviral activities (Table 1).

Based on these results, fraction GLLD-F2 was identified as the most promising fraction against DENV-2 with an IC_{50} value of 1.62 µg/mL and a CC_{50} value of 98.99 µg/mL, resulting in a SI value of 61.10 (Fig. 1). Deep metabolome analysis of molecular networking as a dereplication

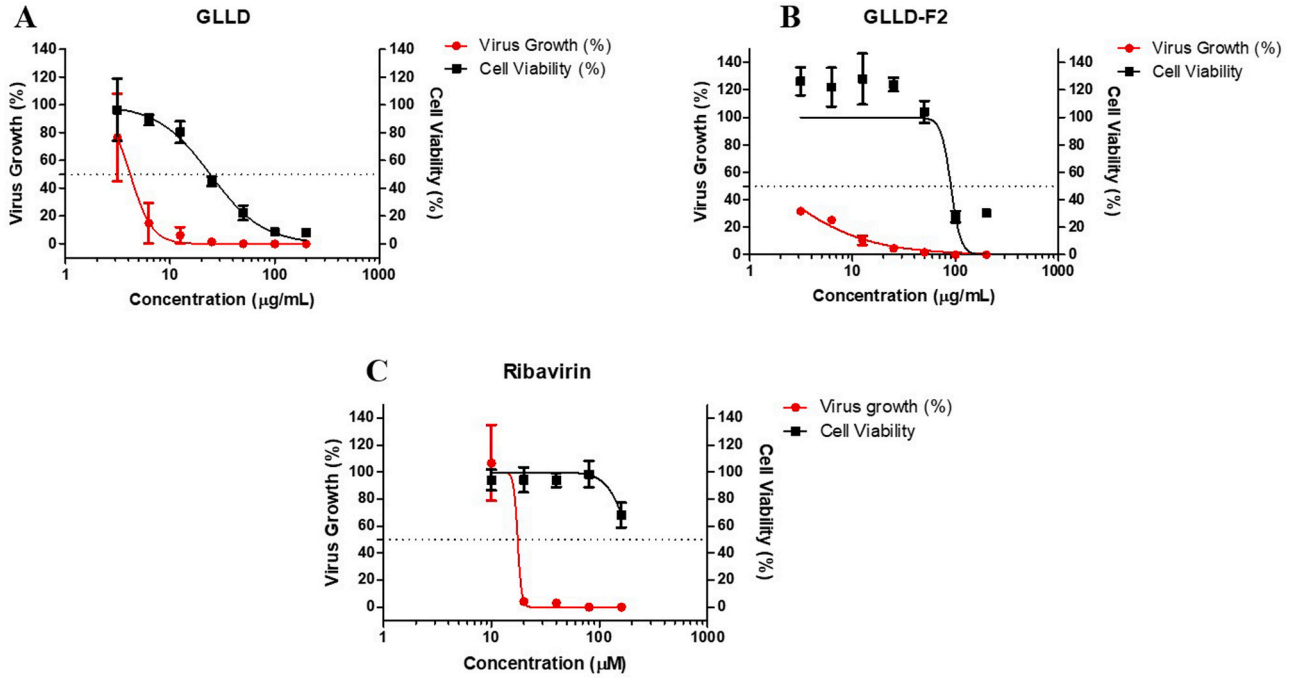

Fig. 1. Dose-response curves showing cytotoxicity and concentration-dependent inhibition of DENV-2 plaque formation for the *G. lanceolatus* extracts (**A**); Dose-response curves showing cytotoxicity and concentration-dependent inhibition of DENV-2 for the fraction GLLD-F2 (**B**); Dose-response curves showing cytotoxicity and concentration-dependent inhibition of DENV-2 plaque formation for the positive control, ribavirin (**C**). Data shown are the mean ± SEM of triplicates from two independent experiments.

Table 1
CC50, IC50, and SI Values for the Anti-dengue Tests of All of the Extracts and Fractions from the GLLD Extract of G. lanceolatus Using Bioassay-guided Fractionation.

Samples	Cytotoxicity CC_{50} (μg/mL)	Plaque assay IC_{50} (μg/mL)	SI
GLLD extracts	24.23 ± 1.14	4.16 ± 1.12	5.82
GLLD-F1	94.90 ± 1.36	8.53 ± 1.36	11.13
GLLD-F2	98.99 ± 1.80	1.62 ± 1.15	61.10
GLLD-F3	8.14 ± 1.07	2.37 ± 1.14	3.43
GLLD-F4	8.27 ± 1.20	2.59 ± 1.14	3.19
GLLD-F5	109.7 ± 1.23	3.51 ± 1.27	31.25
GLLD-F6	152.7 ± 1.20	2.66 ± 1.15	57.41

Data are shown as the mean ± SEM of triplicate assays from two independent experiments.

strategy highlighted that the active fraction F2 is mainly comprised of styryllactones. Thus, further isolation work was focused on this fraction.

3.2. Molecular networking of the active fraction GLLD F2

Following repeated chromatographic separation of GLLD F2, eight styryllactones were unambiguously identified through extensive NMR spectroscopic interpretation (Table S1). Deep metabolome analysis of the biologically active fraction F2 through HR-MS analysis was performed to determine the presence of additional styryllactones. The HR-MS profiling and data-dependent MS/MS data were acquired in the positive ionization mode. The major peaks in the chromatogram (Fig. S1) were identified by matching the retention time and the molecular formula with the isolated compounds (**8**, **11**, **14**, **16**, **17**, **18**, **19**, and **22**) and a reference standard, goniolanceolatin E (**23**), previously isolated from a different part of *G. lanceolatus* (Bihud et al., 2019). The GNPS FB-MN database and the computational annotation tool SIRIUS5 were used to annotate the remaining peaks.

After LCMS processing, the dataset contained 279 MS features was organized into a molecular network (MN) through the application of GNPS FBMN workflow. In addition to the nine styryllactones identified unambiguously and the reference standard, an additional 18 styryllactones were further annotated through *in silico* computation (Table S1). The annotation steps included:1) molecular formula determination; 2) CSI: Finger ID search, which combines molecular fingerprints from MS/MS fragmentation trees and molecular database searches, and 3) chemical family prediction by CANOPUS (Dührkop et al., 2015). Additionally, and to increase the level of confidence in the annotations, a custom molecular database comprising 80 styryllactone derivatives reported from *Goniothalamus* spp. was generated from the *Dictionary of Natural Products* database and submitted to SIRIUS5. The

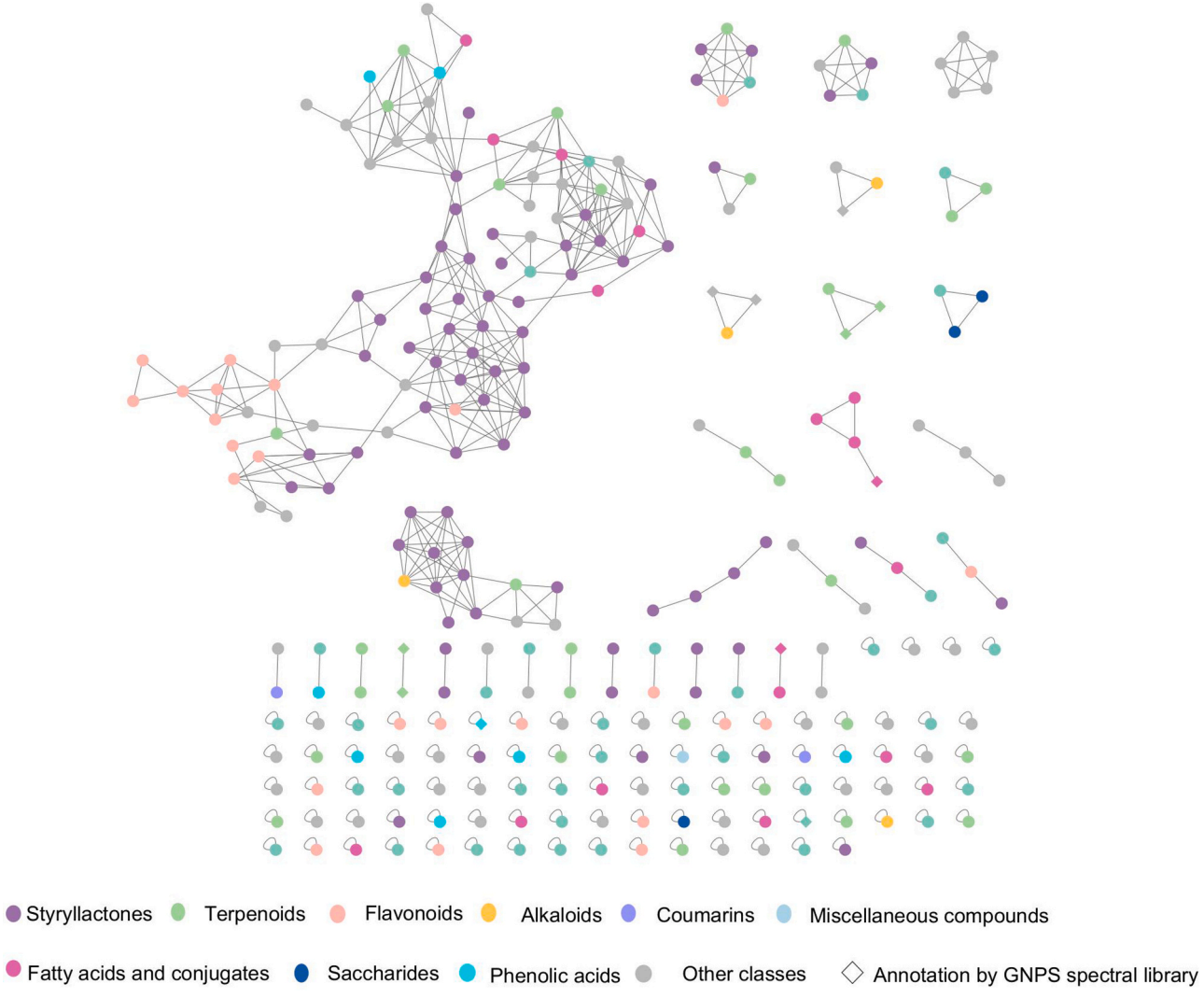

Fig. 2. A molecular network of the 279 MS features from the F2 fraction of the dichloromethane extract of *G. lanceolatus* leaves (GLLD), visualized according to chemical class annotations.

acceptance criteria for annotations were set as a minimum 50% similarity score; note that annotations of isomeric compounds are interchangeable.

The fraction F2 MN consisted of 279 nodes (representing a measured *m/z* at a given retention time), which were grouped into 32 clusters and 91 singletons. Each cluster node is connected by a spectral similarity cosine score. The relationships of all the MS features detected in fraction F2 are presented by the MN, which was visualized according to chemical class (Fig. 2) and chemical structure (Fig. S2) annotations. Fraction F2 was primarily comprised of styryllactones, which were grouped mainly in clusters L1, L2, and L7. Other chemical families (*i.e.*, flavonoids, terpenoids, fatty acids and conjugates, coumarins, saccharides, phenolic acids, miscellaneous compounds, apocarotenoids, naphthalenes, peptides, lipids, macrolides, and organic oxygen compounds) were distributed in smaller clusters and singletons.

The metabolite identification confidence level for all of the annotations is based on the Metabolomics Standards Initiative (MSI) (Schrimpe-Rutledge et al., 2016). Identification at Level 1 is relative to the confirmed structure, either by comparison with reference standards or through NMR structural elucidation of the isolated compounds. Level 2 is for annotation according to MS/MS spectra matching and *in silico* fragments analysis on comparison with the published literature. The Level 3 annotation is for *de novo* structural elucidation involving multiple tentative isomeric candidates. Annotations at Levels 4 and 5 require only a mass formula or an exact mass, respectively (Schrimpe-Rutledge et al., 2016). In this study, annotations were performed at Levels 1 and 3. As a result, 27 styryllactones were annotated from the bioactive fraction, F2. Among the 27 annotations, **22**, **23**, **25**, and **27** were bis-styryllactones and the remaining identified metabolites were monomeric styryllactones.

3.3. Structure elucidation of compound 19

Compound **19** was isolated as a white amorphous solid, $[\alpha]_D^{20}$ + 48.0 (c=0.5, MeOH). with a molecular formula of $C_{14}H_{18}O_5$, as determined through HR-ESI-Orbitrap-MS analysis at *m/z* 289.10590 (calculated 289.10610) $[M+Na]^+$. The infrared (IR) spectrum of **19** showed the broad absorption of a hydroxyl group (OH) at 3413 cm^{-1} , the medium absorption for an alkane group (C-H) at 2947 cm^{-1} , and an ester carbonyl (C═O) at 1734 cm^{-1} .

Further inspection of the ^1H NMR spectroscopic data (Fig. S3) showed the presence of a mono-substituted phenyl moiety from the complex proton resonances in the region δ_H 7.30–7.38 (5 H). Four oxygen-bearing methines were established in the ^1H NMR (δ_H 4.01, 4.12, 4.18, and 4.96) and ^{13}C NMR (δ_C 66.43, 70.52, 67.59, and 75.80) spectra, respectively. In addition, two methylene groups were indicated by the signals at δ_H 1.83 and 1.92/ δ_C 34.41 and δ_H 2.65 and 2.89/ δ_C 40.01, respectively. A methoxy group was present based on the three-proton singlet resonance at δ_H 3.68/ δ_C 51.91. The ^{13}C NMR spectrum also revealed the carbonyl of an aliphatic ester (δ_C 171.83; C-8) and aromatic ring resonances (δ_C 137.63, 127.04, 128.96, and 128.26; for C-1', C-2'/C-6', C-3'/C-5', and C-4'), respectively. A series of COSY correlations (Fig. 3) connecting H-7, H-6, H-5, H-4, H-3, and H-2, suggested that this metabolite has a tetrahydropyran ring. Long-range correlations in the HMBC spectrum from H-2 to C-3/C-4/C-6 and H-5 to C-3/C-4/C-6, C-7, further supported the presence of a tetrahydropyran ring. The monosubstituted phenyl ring is attached to C-2 of the tetrahydropyran ring as evidenced by HMBC correlations between H-2'/H-6' to C-2, and H-2 to C-1'. Similarly, the position of the methyl ester group at C-6 was established based on the HMBC correlations between C-8 to H-7 and H-6 to C-7.

These spectroscopic data of **19** resemble those reported for the known metabolite goniothalesdiol A (Table 2), with notable differences in the chemical shifts and coupling constants involving H-2, H-3, and H-4. A *cis*-1,3-diaxial interaction between H-6 and H-2, as seen in the NOESY experiment established the chair conformation for the tetrahydropyran ring. The vicinal coupling constant of H-2 and H-3 for compound **19** is 4.8 Hz, establishing the axial-equatorial orientation of the respective protons ($H\text{-}2_{ax}$-$H\text{-}3_{eq}$). In goniothalesdiol A, these protons showed an axial-axial orientation with a coupling constant of 8.0 Hz (Lan et al., 2006). Consequently, the orientation of H-4 in the equatorial position can be designated through its coupling with H-3, which is 2.5 Hz, as having an equatorial-equatorial orientation ($H\text{-}3_{eq}$-$H\text{-}4_{eq}$), in contrast to that of goniothalesdiol A ($J_{3,4}$ = 3.6 Hz), where H-3 and H-4 are in axial-equatorial orientation. The equatorial orientation of H-4

Table 2
1HNMR (600 MHz) and ^{13}C NMR (150 MHz) spectral data for **19** in $CDCl_3$ and comparison with the literature data for goniothalesdiol A (δ in ppm and *J*-coupling in Hz)[a].

Position	3-*epi*-Goniothalesdiol A (19)		Goniothalesdiol A (Lan et al., 2006)	
	δ_C	δ_H	δ_C	δ_H
2	75.80	4.96 (1 H, *d*, 4.8)	73.4	4.87 (1 H, *d*, 8.0)
3	66.43	4.01 (1 H, *ddd*, 7.8, 4.8, 2.5)	85.7	3.68 (1 H, *dd*, 8.0, 3.6)
4	67.59	4.18 (1 H, *ddd*, 12.6, 7.8, 2.5)	72.8	4.47 (1 H, *ddd*, 5.6, 3.6, 2.4)
5	34.41	1.83 (1 H, *dt*, 12.6, 7.8) 1.92 (1 H, *dt*, 12.6, 4.8)	39.8	1.77 (1 H, *ddd*, 13.6, 4.8, 2.4) 2.35 (1 H, *ddd*, 13.6, 8.4, 5.6)
6	70.52	4.12 (1 H, *dd*, 7.8, 4.8)	74.4	4.38 (1 H, *dddd*, 8.4, 7.2, 6.4, 4.8)
7	40.01	2.65 (1 H, *dd*, 15.6, 4.8); 2.89 (1 H, *dd*, 15.6, 7.8)	40.3	2.61 (1 H, *dd*, 15.2, 6.4) 2.75 (1 H, *dd*, 15.2, 7.2)
8	171.83	-	172.3	-
8-OCH_3	51.91	3.68 (3 H, *s*)	51.8	3.67 (3 H, *s*)
1'	137.63	-	147.7	-
2', 6'	127.04		126.2	
3', 5'	128.96	7.30-7.38 (5 H, *m*)	128.4	7.28-2.40 (5 H, *m*)
4'	128.26		127.8	

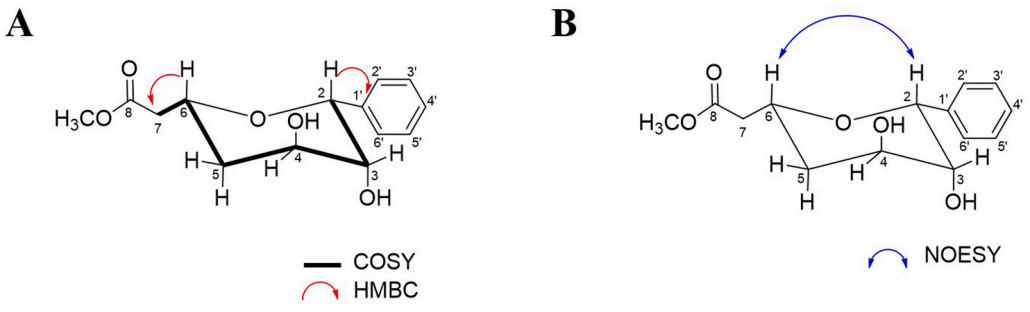

Fig. 3. COSY, HMBC, and NOESY correlations of **19**. COSY, HMBC (**A**); and NOESY correlations (**B**).

corresponds to an *S* relative configuration at C-4, in agreement with the postulation that C-4 of **19** should have the same configuration as C-6 as 6*S*-goniothalamin isolated from the same plant because they have the same biogenetic origin (Rasol et al., 2018). Thus, spectroscopic evidence identified compound **19** as a previously undescribed epimer of goniothalesdiol A, 3-*epi*-goniothalesdiol A, with the relative configurations 2 *R*,3 *R*,4 *S*,6 *R*.

[a]These chemical shift values were compared to the ^{1}H NMR and ^{13}C NMR data of goniothalesdiol A isolated from *G. amuyon* and recorded in $(CD_3)_2OD$ at 400 MHz (Lan et al., 2006).

3.4. In vitro antiviral assay

Eight metabolites derived from GLLD-F2 were subjected to the dose-dependent plaque reduction assay using MTT to evaluate their antiviral activity. Among these, goniolanceolatin A (**22**) showed the most promising results with an IC_{50} value of 6.63 μM, a CC_{50} value of 26.90 μM, and a SI value of 4.06 (Table 3). Ribavirin was used as a positive control in the test with an IC_{50} value of 17.52 μM.

Data shown are the mean ± SEM of triplicate assays from two independent experiments.

3.5. Quantitative viral load by real-time qPCR

To confirm the aforementioned observations, quantitative real-time PCR was used to determine the viral load of DENV-2 in infected cells after treatment with goniolanceolatin A (**22**). The data were confirmed by quantification of the viral RNA. The results showed that **22** reduced the viral RNA in a dose-dependent manner (Fig. 4). In parallel with the plaque assay data, **22** showed an IC_{50} value of 5.07 μM, a CC_{50} value of 26.90 μM, and an SI value of 5.30 against DENV-2. The RT-qPCR result for **22** against DENV-2 was different from the plaque assay since the PCR assay reflects the detection of both live and dead viral RNA, while the plaque assay only detects the infectious viruses that can form plaque. However, comparative analysis between the plaque assay and RT-qPCR showed no significant difference in estimating the virus titer.

3.6. Docking analysis

A styryl pyrone derivative (SPD) isolated from *G. umbrosus* was reported to inhibit the activity of the E protein in the DENV-2 replication cycle *in vitro* and *in silico* (Abd Wahab et al., 2022). Glycoprotein E in DENV-2, which can interact with several cell molecules, is the most crucial protein during the viral entry to host cells, and the clathrin-intermediate endocytosis process. Thus, the E protein is considered the most suitable target for the development of anti-dengue agents (Abd Wahab et al., 2022). In this study, the styryllactone derivatives isolated from fraction F2 of the bioactive GLLD extract of *G. lanceolatus* were docked against the target E protein (1OKE). The validation process was achieved through re-docking of the co-crystalline ligand selected from the crystallographic protease structure into the same protease binding

Table 3
CC_{50}, IC_{50}, and SI values for the anti-DENV tests of all isolated compounds derived from GLLD F2 through bioassay-guided fractionation.

Compounds	Cytotoxicity CC_{50} (μM)	Plaque assay IC_{50} (μM)	SI
8	54.87 ± 1.11	> 250	< 1
11	> 250	> 250	< 1
14	> 250	> 250	< 1
16	> 250	> 250	< 1
17	195.4 ± 1.77	> 250	< 1
18	> 250	84.24 ± 1.86	2.97
19	> 250	> 240	< 1
22	26.90 ± 1.16	6.63 ± 1.22	4.06

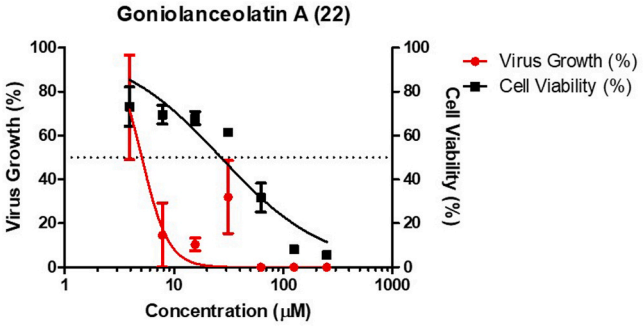

Fig. 4. RT-qPCR results for **22** against DENV-2. Data shown are the mean ± SEM of triplicate assay from two independent experiments.

pocket. Based on the results, the RMSD value (1.16 Å) recorded for 1OKE was below the 2.0 Å threshold (Modis et al., 2003; Benarroch et al., 2004; Noble et al., 2013).

Compound **22** binds at domain III of the E protein and was considered to have very favourable interactions with the proteases due to the excellent docking energy interaction value and a high number of critical interactions with the active site residues. This result was supported by an *in vitro* test in which **22** exhibited activities against DENV-2 with an SI value of 4.06. The result suggests that **22** could bind to the active site of the E DENV protein with a docking energy interaction value of − 35.6 kcal/mol (Fig. 5). In this way, **22** may prevent or significantly interfere with the initial attachment process of the viral particles to the host cell receptors (Djoumbou-Feunang et al., 2019). The hydroxyl group of **22** forms a conventional hydrogen bond (C═O—H-O) with the backbone oxygen of residue Gln271 (2.59 Å). The ligand-enzyme complex with **22** was also stabilized by a hydrogen bond interaction with Gly275 at 2.50 Å (Table S3) and through hydrophobic interactions with the amino acids Leu277 and Lys47. Based on the molecular docking results, it is known that **22** presented a lower binding interaction energy (−35.6 kcal/mol) compared to the reference control ribavirin (−31.3 kcal/mol). Compound **22** also had similar binding residues to ribavirin. Interaction with the same amino acid residue, Leu277 (Table S3), indicated that **22** could potentially induce biological effects on the target protein.

Based on previous studies, an extensive computational assessment was performed on all styryllactone derivatives in the *Dictionary of Natural Products* (DNP) database to identify potential strong binding compounds against several DENV-2 targets (Abdullah et al., 2022). All of the top ten ranked compounds belonged to the bis-styryllactone series, and interestingly, the isolated bis-styryllactone **22** was predicted to be one of the top ten ranked compounds. These data support compound **22** for consideration as a candidate for further evaluation as an anti-DENV-2 metabolite of interest.

4. Conclusions

In summary, one new styryllactone **19** and seven known styryllactones (**8**, **11**, **14**, **16**, **17**, **18**, and **22**) were isolated during a bioactivity-directed, phytochemical analysis of the dichloromethane extract fraction F2 from the leaves of *G. lanceolatus*. The new compound **19** differs from the previously reported goniothalesdiol A in the absolute stereochemistry at position C-3 which was proposed as (2 *R*,3 *R*,4 *S*,6 *R*) and was named as 3-*epi*-goniothalesdiol A. *In vitro* evaluation showed that compound **22** had promising anti-dengue viral activity displaying inhibition of the production of infectious viral particles experimentally, namely the plaque reduction assay with the highest SI value of 4.06 and by qRT-PCR with an SI value of 5.30. *In silico* docking studies revealed that **22** has favourable interactions with the crucial amino acids of the DENV-2 Envelope proteins with excellent docking energy interaction value and several critical interactions with the active site residues,

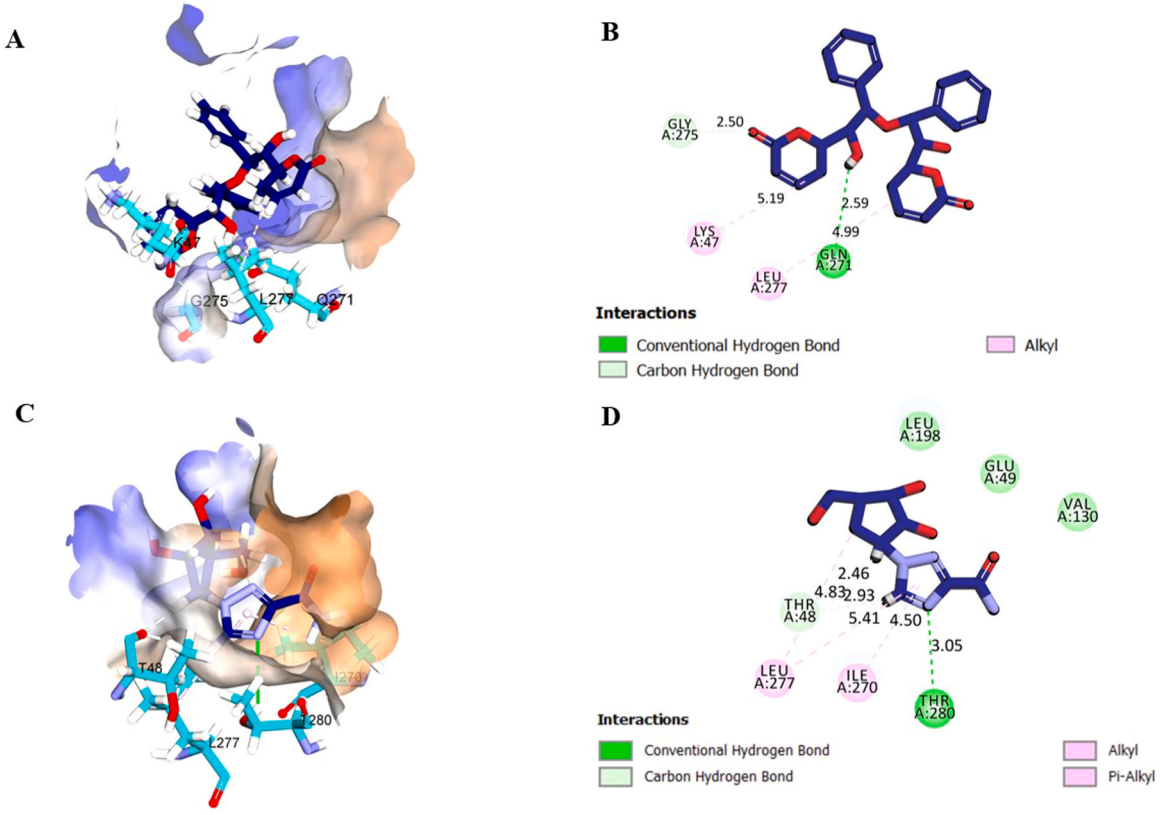

Fig. 5. 3D-Interactions of **22** with the envelope DENV protein (PDB 1OKE) (**A**); 2D-Interactions of **22** with the envelope DENV protein (PDB 1OKE) (**B**); 3D-Interactions of ribavirin (control) with the envelope DENV protein (PDB 1OKE) (**C**); and 2D-Interactions of ribavirin (control) with the envelope DENV protein (PDB 1OKE) (**D**).

comparable to ribavirin. As demonstrated in this study, bioprospecting remains beneficial for identifying antiviral compounds of potential interest. In addition, the essential interrelationship between *in vitro* and *in silico* evaluations fostered the identification of an antiviral compound while excluding others effectively, and predicted the mechanism of action.

Declaration of Competing Interest

The authors declare no conflict of interest.

Data Availability

Data will be made available on request.

Acknowledgments

The authors would like to acknowledge the Ministry of Higher Education of Malaysia for providing a grant under the Fundamental Research Grant Scheme, [FRGS 1/2021/STG04/UITM/01/2)], and [UiTM600-IRMI/FRGS 5/3 (111/2019)].

Appendix A. Supporting information

Supplementary data associated with this article can be found in the online version at doi:10.1016/j.phytol.2024.01.012.

References

Abd Wahab, N.Z., Ibrahim, N., 2022. Styrylpyrone derivative (SPD) extracted from.
Abdullah, N.N., Imran, S., Lam, K.W., Ismail, N.H., 2022. Computational screening of styryl lactone compounds isolated from *Goniothalamus* species to identify potential inhibitors for dengue virus. J. Comput. Biophys. Chem. 21, 821–843.
Abdullah, N.N., Afzan, A., Jelas, N.H., Mohd Abdul Razak, M.R., Nur Syaidatul, Rasol, N. E., Bihud, N.V., Zainol, M., Ahmad, F.B., Abdullah, F., Ismail, N.H , 2021. Dereplication of a dichloromethane extract of Goniothalamus lanceolatus leaves using UHPLC-ESI-Orbitrap HRMS. Malays. J. Chem. 23, 103–114.
Benarroch, D., Egloff, M.P., Mulard, L., Guerreiro, C., Romette, J.L., Canard, B., 2004. A structural basis for the inhibition of the NS5 dengue virus mRNA 2′-*O*-methyltransferase domain by ribavirin 5′-triphosphate. J. Biol. Chem. 279, 35638–35643.
Bihud, N.V., Rasol, N.E., Imran, S., Awang, K., Ahmad, F.B., Mai, C.W., Ismail, N.H., 2019. Goniolanceolatins A–H, cytotoxic bis-styryllactones from *Goniothalamus lanceolatus*. J. Nat. Prod. 82, 2430–2442.
Böcker, S., Dührkop, K., 2016. Fragmentation trees reloaded. J. Chemin. 8, 5.
Burleson, F.G., Chambers, T.M., Wiedbrauk, D.L., 1992. Virology: A Laboratory Manual. Academic Press, San Diego, CA, pp. 39–44.
Cao, S.G., Wu, X.H., Sim, K.Y., Tan, B.K.H., Pereira, J.T., Goh, S.H., 1998. Styryl-lactone derivatives and alkaloids from *Goniothalamus borneensis* (Annonaceae).Tetrahedron 54, 2143–2148.
Claire, L., Melodie, B., Karren, D.B., Anthony, R.C., Frederic, M., Vanida, C., Rohan, A.D., 2013. *In vivo* antiplasmodial and toxicological effects of *Goniothalamus lanceolatus* crude extracts. Phytochemistry 86, 121–126.
Djoumbou-Feunang, Y., Pon, A., Karu, N., Zheng, J., Li, C., Arndt, D., Gautam, M., Allen, F., Wishart, D.S., 2019. CFM-ID 3.0: significantly improved ESI-MS/MS prediction and compound identification. Metabolites 9, 72.
Dührkop, K., Shen, H., Meusel, M., Rousu, J., Böcker, S., 2015. Searching molecular structure databases with tandem mass spectra using CSI:FingerID. Proc. Natl. Acad. Sci. 112, 12580–12585.
Ferris, M.M., Stepp, P.C., Ranno, K.A., Mahmoud, W., Ibbitson, E., Jarvis, J., Rowlen, K. L., 2011. Evaluation of the Virus Counter® for rapid baculovirus quantitation. J. Virol. Methods 171, 111–116.
Gubler, D.J., 1998. Dengue and dengue hemorrhagic fever. Clin. Microbiol Rev. 11.
Gurukumar, K.R., Priyadarshini, D., Patil, J.A., Bhagat, A., Singh, A., Shah, P.S., Cecilia, D., 2009. Development of real-time PCR for detection and quantitation of dengue viruses. Virol. J. 6, 10.
Ichino, C., Soonthornchareonnon, N., Chuakal, W., Kiyohara, H., Ishiyama, A., Sekiguchi, H., Namatame, M., Otoguro, K., Omura, S., Yamada, H., 2006. Antimalarial activity of biflavonoids from *Ochna integerrima*. Phytother. Res. 20, 307–309.
Kaharudin, F.A., Zohdi, R.M., Mukhtar, S.M., Sidek, H.M., Bihud, N.V., Rasol, N.E., Ismail, N.H., 2020. *In vitro* antiplasmodial and cytotoxicity activities of crude extracts and major compounds from *Goniothalamus lanceolatus*. J. Ethnopharmacol. 254, 112657.

Kalayanarooj, S., 2011. Clinical manifestations and management of dengue/DHF/DSS Trop. Med. Health. 39, 83–87.
Kwon, H.J., Kim, H.H., Yoon, S.Y., Ryu, Y.B., Chang, J.S., Cho, K.O., Rho, M.C., Park, S. J., Lee, W.S., 2010. *In vitro* inhibitory activity of *Alpinia katsumadai* extracts against influenza virus infection and hemagglutination. Virol. J. 7, 307.
Lan, Y.H., Chang, F.R., Yang, Y.L., Wu, Y.C., 2006. New constituents from stems of *Goniothalamus amuyon*. Chem. Pharm. Bull. 54, 1040–1043.
Likhitwitayawuid, K., Angerhofer, C.K., Cordell, G.A., Pezzuto, J.M., Ruangrungsi, N., 1993. Cytotoxic and antimalarial bisbenzylisoquinoline alkaloids from *Stephania erecta*. J. Nat. Prod. 56, 30–38.
Mahiwan, C., Buayairasaka, M., Nuntasaen, N., Meepowpan, P., Pompimon, W., 2013. Potential cancer chemopreventive activity of styryllactones from *Goniothalamus marcanii*. Am. J. Appl. Sci.. 10, 112–116.
Mashudi, D.N., Ahmad, N., Mohd Said, S., 2022. Level of dengue preventive practices and associated factors in a Malaysian residential area during the COVID-19 pandemic: a cross-sectional study. PloS One 17, 1–15.
Modis, Y., Ogata, S., Clements, D., Harrison, S.C., 2003. A ligand-binding pocket in the dengue virus envelope glycoprotein. Proc. Natl. Acad. Sci. 100, 6986–6991.
Noble, C.G., Lim, S.P., Chen, Y.L., Liew, C.W., Yap, L., Lescar, J., Shi, P.Y., 2013. Conformational flexibility of the dengue virus RNA-dependent RNA polymerase revealed by a complex with an inhibitor. J. Virol. 87, 5291–5295.
Nothias, L.F., Nothias-Esposito, M., da Silva, R., Wang, M., Protsyuk, I., Zhang, Z., Dorrestein, P.C., 2018. Bioactivity-based molecular networking for the discovery of drug leads in natural product bioassay-guided fractionation. J. Nat. Prod.. 81, 758–767.
Paz-Bailey, G., Adams, L., Wong, J.M., Poehling, K.A., Chen, W.H., McNally, V., Atmar, R.L., Waterman, S.H., 2021. Dengue vaccine. Recomm. Advis. Comm. Immun. Pract. Morb. Mortal. Wkly. Rep. 70, 1–16.
Prawat, U., Chaimanee, S., Butsuri, A., Salae, A.W., Tuntiwachwuttikul, P., 2012. Bioactive styryllactones, two new naphthoquinones and one new styryllactone, and other constituents from *Goniothalamus scortechinii*. Phytochem. Lett. 5, 529–534.
Rasol, N.E., Ahmad, F.B., Mai, C.W., Bihud, N.V., Abdullah, F., Awang, K., Ismail, N.H., 2018. Styryl lactones from roots and barks of *Goniothalamus lanceolatus*. Nat. Prod. Commun. 13, 1575–1578.
Schrimpe-Rutledge, A.C., Codreanu, S.G., Sherrod, S.D., McLean, J.A., 2016. Untargeted metabolomics strategies-challenges and emerging directions. J. Am. Soc. Mass Spectrom. 27, 1897–1905.
Severson, W.E., McDowell, M., Ananthan, S., Chung, D.H., Rasmussen, L., Sosa, M.I., Jonsson, C.B., 2008. High-throughput screening of a 100,000-compound library for inhibitors of influenza A virus (H3N2). J. Biomol. Screen. 13, 879–887.
Shannon, P., 2003. Cytoscape: a software environment for integrated models of biomolecular interaction networks. Genome Res 13, 2498–2504.
Trujillo-Correa, A.I., Quintero-Gil, D.C., Diaz-Castillo, F., Quiñones, W., Robledo, S.M., Martinez-Gutierrez, M., 2019. *In vitro* and *in silico* anti-dengue activity of compounds obtained from *Psidium guajava* through bioprospecting. BMC Complement. Altern. Med. 19, 298–314.
Wiart, C., 2007. Cytotoxic activity of acetogenins and styryllactones isolated from *Goniothalamus undulatus* Ridl. root extracts against a lung cancer cell line (COR-L23). Evid. -based Complement. Altern. Med. 4, 299–311.
Wu, G., Robertson, D.H., Brooks, C.L., Vieth, M., 2003. Detailed analysis of grid-based molecular docking: A case study of CDOCKER-A CHARMm-based MD docking algorithm. J. Comput. Chem. 24, 1549–1562.
Yang, Z., Li, J., Chen, X., Zhao, X., Wang, Y., 2022. Deciphering bioactive compounds of complex natural products by tandem mass spectral molecular networking combined with an aggregation-induced emission-based probe. J. Pharm. Anal.. 12, 129–135.
Yasuhara-Bell, J., Yang, Y., Barlow, R., Trapido-Rosenthal, H., Lu, Y., 2010. In vitro evaluation of marine-microorganism extracts for anti-viral activity. Virol J. 7, 182.
Zandi, K., Taherzadeh, M., Yaghoubi, R., Tajbakhsh, S., Rastian, Z., Sartavi, K., 2009. Antiviral activity of *Avicennia marina* against herpes simplex virus type 1 and vaccine strain of poliovirus (an *in vitro* study). J. Med. Plant Res 3, 771–775.